



Identification of key genes and enzymes contributing to nutrition conversion of *Torreya grandis* nuts during post-ripening process

Lili Song¹, Xuecheng Meng¹, Lei Yang¹, Zhenmin Ma, Minying Zhou, Chenliang Yu, Zuying Zhang, Weiwu Yu, Jiasheng Wu^{*}, Heqiang Lou^{*}

State Key Laboratory of Subtropical Silviculture, Zhejiang A&F University, Hangzhou, Zhejiang 311300, China

ARTICLE INFO

Keywords:

Torreya grandis
Nutrition conversion
Transcriptome
Enzyme activity
Post-ripening

ABSTRACT

The seeds of *Torreya grandis* are necessary to go through a ripening process, which eventually leads to nutrition conversion and the production of edible nuts. However, the molecular basis of nutrition conversion remains unclear. Here, transcriptome sequencing was performed on seeds treated with different temperature and humidity. A total of 881 unigenes related to nutrition conversion were identified. The correlations between nutrient content and gene expression suggested that sucrose phosphate synthase (SPS), dihydrolipoyllysine-residue succinyltransferase component of 2-oxoglutarate dehydrogenase complex (DLST), glycerol-3-phosphate acyltransferase (GPAT) and Pyruvate kinase (PK) may play key roles in nutrition conversion. Transient over-expression of *TgDLST*, *TgPK* and *TgGPAT* in tobacco leaves promoted nutritional conversion. Moreover, enzyme activity analysis indicated that diacylglycerol acyltransferase (DGAT) and pyruvate dehydrogenase (PDH) activities may also accelerate the nutritional conversion. This study uncovers the molecular basis of nutrition conversion in *T. grandis* seeds, which critical for shortening the time of nutrition conversion.

1. Introduction

Torreya grandis (*T. grandis*) is a large evergreen tree which belongs to *Taxaceae* family and is cultivated as the rare economic tree in China. Its seeds generally take 2–3 years to mature (Ni & Shi, 2014). *T. grandis* seed presents high nutritional value and medicinal effects due to its high contents of tocopherols, crude fiber, squalene, sitosterol, fatty acids, protein and triacylglycerol (Lou et al., 2019; Saeed et al., 2007; Suo et al., 2019). Different from other nuts, *T. grandis* seeds must go through a special post-ripening process, which results in the production of edible nuts. The post-ripening exists in many food crops and fruits, such as wheat, sunflower and soybean (Bazin et al., 2011; Wu et al., 2017). It was reported that the post-ripening process directly affects several metabolic changes of seeds, such as ethylene synthesis, cell wall metabolism, starch and organic acid conversion, and soluble sugar, lipid, and amino acid accumulation (4–6). Therefore, the post-ripening process plays a vital role in the quality and nutritional value of *T. grandis* nuts and many other crops and fruits.

It has been found that some environmental conditions could dramatically affect seed quality during post-ripening process. The

quality of nuts influenced by temperature and humidity owns to lipid peroxidation (Onilude et al., 2010). Reports have suggested that the nutrient conversion and the oil accumulation are closely related to the treatment time, temperature and humidity (Ye et al., 2017). It has been showed that temperature resulted in increase of fatty acids and decrease of bioactive compounds and antioxidants (Chapman & Onlogge, 2012).

In higher plants, the metabolic pathway involved in nutrition conversion during the ripening stage includes sugar metabolism, oil and amino acid synthesis. Starch is hydrolyzed to soluble sugars which are then converted to fatty acids, glycerol phosphate and amino acids, subsequently produced fats and proteins by a set of enzymes. The post-ripening is typically accompanied by the depolymerization and solubilization of various classes of cell wall polysaccharides, such as pectins and hemicelluloses, as well as by an increase in the expression levels of genes, proteins, and enzyme activities related to sugar metabolism (Giovannoni, 2001; Rose et al., 2000). The changes of starch content were mainly caused by polymerization during storage (Pongsawatmanit et al., 2006) or hydrolysis of amylase (Zhou et al., 2003). Reports have suggested that ADP-glucose pyrophosphorylase (AGPaes) was the limiting enzyme of the starch synthesis pathway, involved in the first

^{*} Corresponding authors.

E-mail addresses: wujs@zafu.edu.cn (J. Wu), 20170030@zafu.edu.cn (H. Lou).

¹ These authors contributed equally to this work.

reaction of starch synthesis (Wang et al., 2017). The synthesis of amylose and amylopectin were catalyzed by granule-bound starch synthase (GBSS) and soluble starch synthase (SSS), respectively. Reports have suggested that the invertase (IVR) and sucrose synthase (SS) in tomato were closely related to content of sugar (Yuan et al., 2009). SS and sucrose phosphate synthase (SPS) were mainly responsible for the accumulation of sugar in peach (Lombardo et al., 2011). The fatty acids (FA) biosynthesis first occurs in plastid by a series of reactions, including condensation, reduction and dehydration with the participation of FA synthases (Xu & Shanklin, 2016). In plants, it was found that the key enzymes of lipid synthesis were acetyl-CoA carboxylase (ACCase), acyl-CoA thioesterases (FATA and FATB), 3-ketoacyl-ACP synthase (KAS), glycerol-3-phosphate acyltransferase (GPAT) and diacylglycerol acyltransferase (DGAT) (Ding et al., 2020; Stéphane et al., 2013). Triacylglycerol (TAG) is the main storage fat of the most oil seeds which is synthesized mainly in the plastid of plant. DGAT catalyzes the last step of TAG synthetic pathway, which is a rate-limiting enzyme of this pathway (Guihéneuf et al., 2011).

In our previous study, we carried out different temperature and humidity treatments on seeds of *T. grandis* and concluded the effective treatment condition for nutrition conversion (Zhang et al., 2020). It was found that 20 °C combined with 90% relative humidity was the best treatment. However, the key enzymes and genes for nutrition conversion of *Torreya grandis* nuts during post-ripening process remains unknown. In this study, we further performed transcriptome sequencing on the treated seeds to uncover the molecular basis of nutrition conversion. Metabolism pathway of nutrition conversion of *T. grandis* was identified by the transcriptome sequencing data and previous studies. Pearson correlation analysis between the transcript abundance of pathway genes and the content of starch, soluble sugars, soluble protein and oil was conducted to identify potential key genes. Amino acid sequence alignment analysis was used to characterize the candidate genes for nutrition conversion. The function of the candidate genes was verified by transient over-expression analysis in tobacco leaves. Moreover, we also measured the activities of enzymes in the nutrition conversion pathway.

2. Materials and methods

2.1. Plant materials

This study was carried out using the samples from our previous study (Zhang et al., 2020). *T. grandis* seeds were placed in thermostats (35 cm × 35 cm × 15 cm cube for each). Four treatments were set as follows: T20-LH (20 °C ± 2 °C and 70% RH), T30-LH (30 °C ± 2 °C and 70% RH), T20-HH (20 °C ± 2 °C and 90% RH) and T30-HH (30 °C ± 2 °C and 90% RH). These treated samples were used for illumina sequencing and enzyme activity determination in this study.

2.2. RNA extraction, cDNA library construction, and illumina sequencing

The total RNA was extracted from kernels of *T. grandis* using RNeasy Plant MiniKit (QIAGEN). Then the cDNA library construction and illumina sequencing were performed by Hangzhou Hanyu Biotechnology Co. Ltd. (Hangzhou, China). The mRNA with polyA structure was isolated using oligo (dT) magnetic beads from the total RNA. Subsequently, the RNA was broken into 200–300 bp fragments that were used as templates for cDNA synthesis. Afterwards 6-base random primers and reverse transcriptase was used to synthesis the first-strand cDNA, which was the template for the second strand cDNA synthesis. After library construction, the library fragments were enriched by PCR amplification, and then library was screened according to the fragment size (ranging from 300 to 400 bp). Then, the quality of the library was assessed using Agilent 2100 Bioanalyzer, and then the total concentration and the effective concentration of the library were tested. Libraries with different Index sequences were then mixed proportionally. The resulting cDNA library was sequenced using the Illumina HiSeq™ 2000

sequencing platform.

2.3. Transcriptome data analysis

High-quality reads were obtained after filtering the original sequencing data by the fastp software and was *de novo* assembled by splicing high-quality sequencing data with Trinity. The transcripts were annotated using five public databases (NR, GO, KEGG, eggNOG and Swissprot) with an E-value ≤ 10⁻⁵. The similarity between the gene sequences of *T. grandis* and related species was obtained. The differential expression of the samples was analyzed using the DESeq2 software. The false discovery rate (FDR) was obtained by using the Benjamin–Hochberg method to correct the hypothesis test probability (*P* value). The screening criteria for differential gene were FDR ≤ 0.05 and the |log₂-ratio| ≥ 1. BLAST software was used to compare cDNA or protein sequences to the KEGG database to obtain the KO number of the genes, and then, the KEGG pathways for the genes were determined with a corrected *P*-value < 0.05.

2.4. Quantitative real-time PCR (qRT-PCR)

Total RNA used for qRT-PCR was isolated using RNeasy Plant MiniKit (QIAGEN). The first-strand cDNA was synthesized from total RNA using the Reverse Transcription Kit (PrimeScript™ RT Master Mix, Takara). The qRT-PCR was performed with a C1000 Touch™ Thermal Cycler system (Bio-Rad) and the ChamQ SYBR qPCR Master Mix kit (Vazyme). The reaction conditions were as follows: 95 °C for 5 min followed by 45 cycles of 95 °C for 10 s, 55 °C for 10 s, and 72 °C for 15 s. The primer pairs of each gene were listed in Table S1. Relative transcript abundance was calculated by 2^{-ΔΔCt} method. The actin gene was used to standardize gene expression. Ct represents the reaction cycle number at which the amount of target reaches a fixed threshold.

2.5. Transient expression of candidate genes in *Nicotiana benthamiana* leaves

The full-length cDNA of candidate genes were amplified from cDNA using PrimeSTAR® HS (Premix, Takara), and introduced into the binary vector 35S::GFP (modified from pCambia1300) using a ClonExpress®II One Step Cloning Kit (Vazyme, China). Primers used are listed in Table S1. All resulting constructs were transformed into *Agrobacterium tumefaciens* strain GV3101. The Agrobacteria containing these constructs were grown in LB media which contains 50 mg/L kanamycin until OD₆₀₀ reached to 0.5 at 28 °C. After centrifugation at 6000 rpm for 5 min, the supernatants were removed and the agrobacteria were resuspended in infiltration buffer (10 mM MgCl₂, 0.1 mM acetosyringone, and 10 mM MES). For transient expression of the candidate proteins, the suspensions were then injected into young leaves of *Nicotiana benthamiana* by syringes without a needle. After 72 h incubation, the leave samples were harvested and stored at -80 °C until further analysis.

2.6. Determination of oil, soluble sugar, soluble protein and starch contents

The oil content determination was referred to the method reported by Zhang et al. (2020). The samples were ground into powder and dried at 60 °C for 24 h. 10 g dried samples were extracted with 200 mL of petroleum ether at 45 °C in a water bath for about 8–12 h, and then dried to constant weight after defatting.

The nut residue was used for the determination of soluble sugar, starch and soluble protein. Soluble sugar and starch were measured based on the methods used by Zhang et al. (2020). 10 mL of alcohol (80%) was mixed with 0.5 g nut residue, and then reacted in a water bath at 80 °C for 60 min. After centrifuged (4000 rpm for 15 min), the supernatant was collected for soluble sugar determination. Before

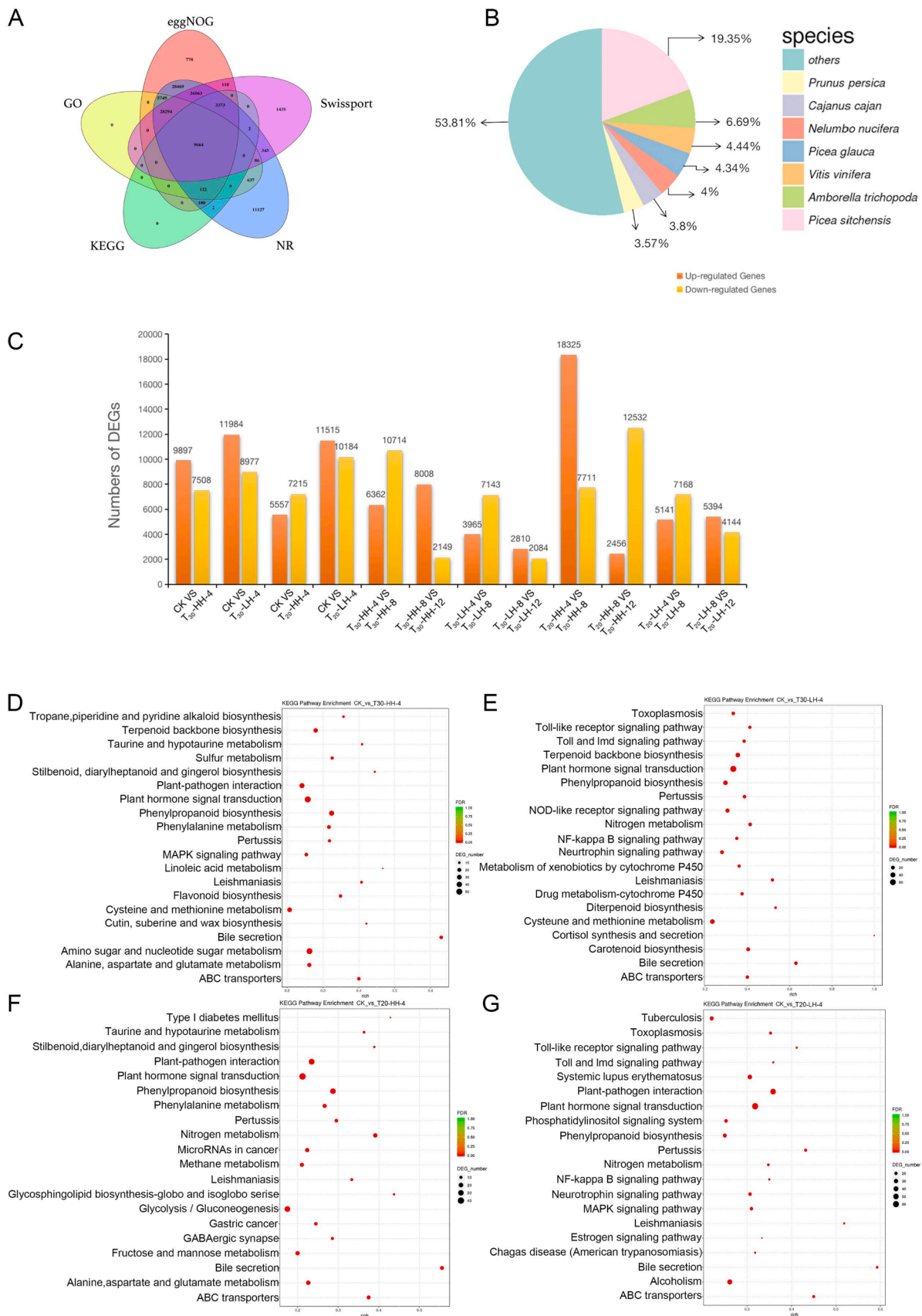
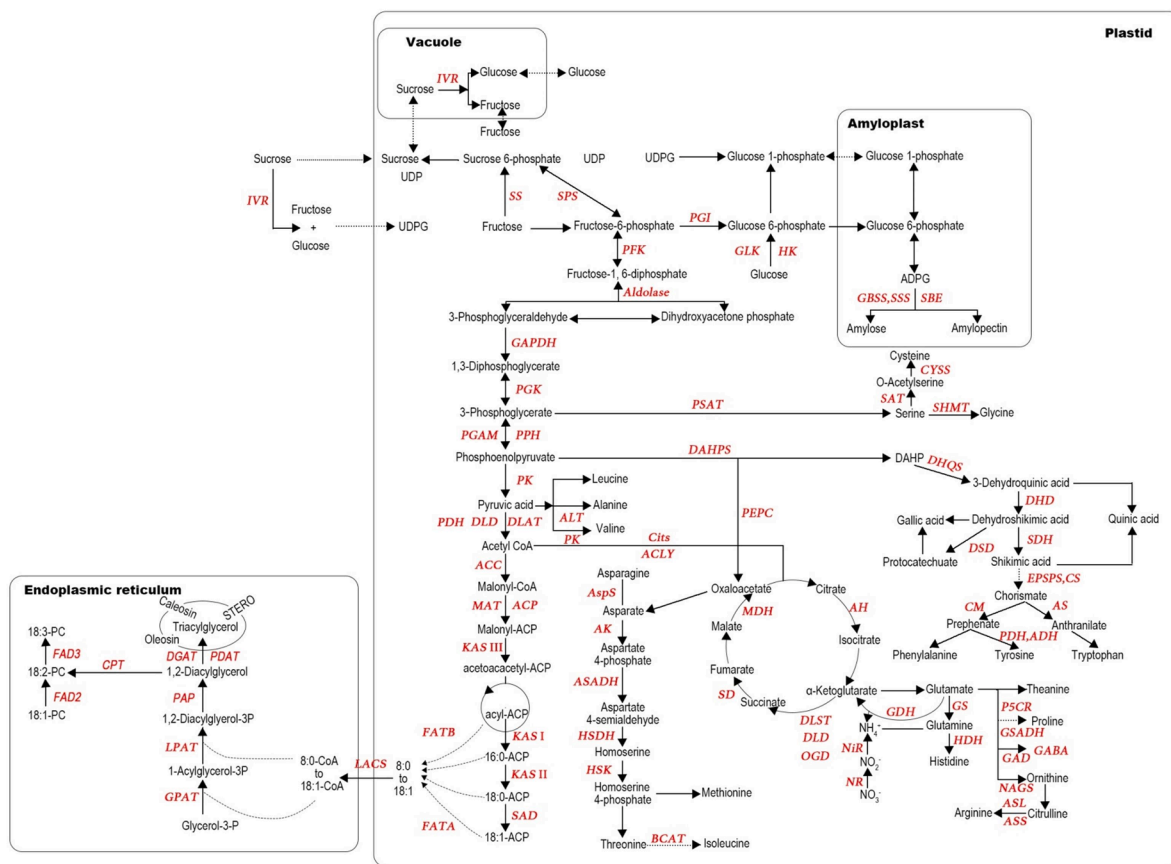
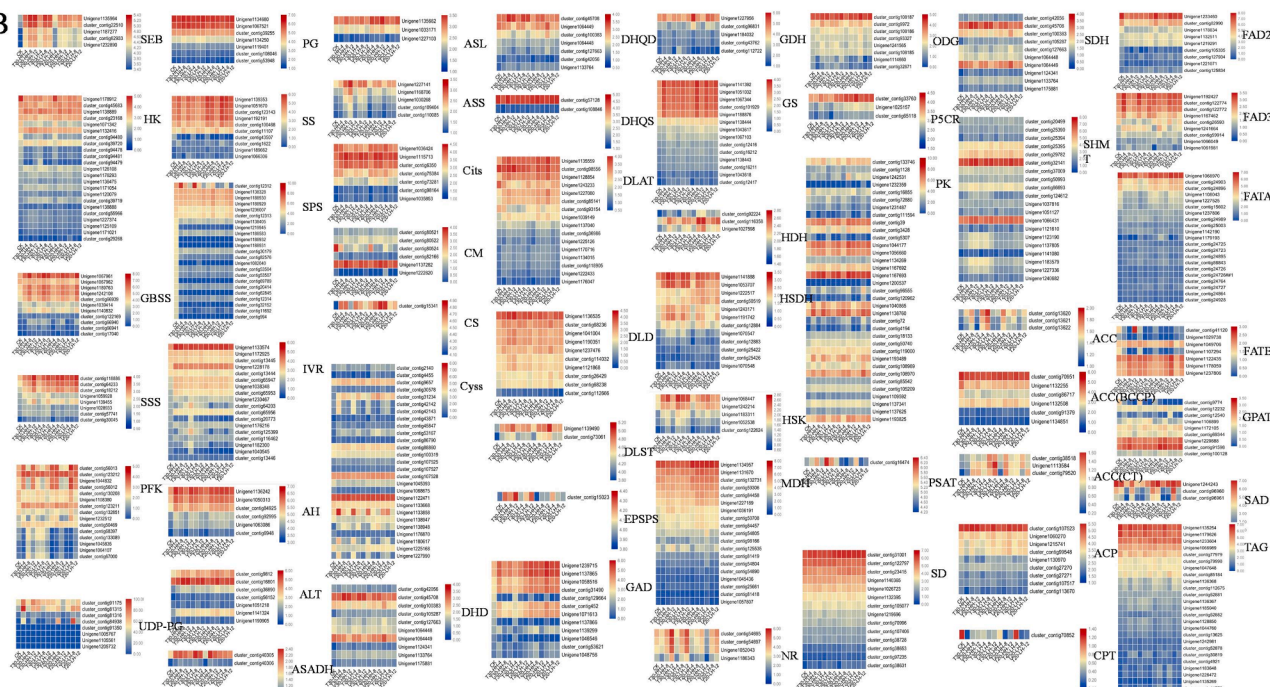


Fig. 1. Characteristics of homology search of unigenes. (A) Venn diagram of number of unigenes annotated by BLASTx. Numbers in the circles indicated the number of unigenes annotated by single or multiple databases. (B) Category of NR annotation. Diagram of percent of unigenes annotated by BLASTx. (C) The number of up and down-regulated unigenes in different comparison groups. (D) The top 20 KEGG pathways of CK_vs_T30-HH-4 DEGs. (E) The top 20 KEGG pathways of CK_vs_T30-LH-4 DEGs. (F) The top 20 KEGG pathways of CK_vs_T20-HH-4 DEGs. (G) The top 20 KEGG pathways of CK_vs_T20-LH-4 DEGs.

A



B



(caption on next page)

Fig. 2. Proposed nutrition conversion pathway (A) and temperature and humidity responsive patterns of genes involved in the nutrition conversion pathway (B). PFK, phosphofructokinase; HK, hexokinase; SPS, sucrose phosphate synthase; SS, sucrose synthase; IVR, invertase; PG, phosphoglucomutase; UDP-GP, UDP-glucose pyrophosphorylase; GK, glucokinase; GBSS, granule-bound starch synthase; SSS, soluble starch synthase; SBE, starch branching enzyme; ACC, acetyl-CoA carboxylase; ACP, acyl carrier protein; FATA, acyl-ACP thioesterase A; FATB, acyl-ACP thioesterase; KAS, ketoacyl-ACP synthase; SAD, stearoyl-ACP desaturase; GPAT, glycerol-3-phosphate acyltransferase; LPAT, lysophosphatidic acid acyltransferase; FAD2, v-6 desaturase; FAD3, v-3 desaturase; CPT, phosphatidylcholine:diacylglycerol cholinephosphotransferase; PK, pyruvate kinase; PAST, phosphoserine aminotransferase; CM, chorismate mutase; CS, chorismate synthase; DHD, 3-dehydroquinate dehydratase; DHQS, 3-dehydroquinate synthase; EPSPS, 3-phosphoshikimate 1-carboxyvinyltransferase; SDH, shikimate dehydrogenase; ALT, alanine transaminase; CysS, cysteine synthase; SHMT, serine hydroxymethyltransferase; DLD, dihydrolipoyl dehydrogenase; DLAT, dihydrolipoyllysine-residue acetyltransferase; MDH, malate dehydrogenase; CITS, citrate synthase; AH, aconitate hydratase; ODG, 2-oxoglutarate dehydrogenase; DLST, Dihydrolipoyllysine-residue succinyltransferase component of 2-oxoglutarate dehydrogenase complex; PEPC, Phosphoenolpyruvate carboxylase; SD, Succinate dehydrogenase; ASADH, aspartate-semialdehyde dehydrogenase; HSDH, homoserine dehydrogenase; HSK, homoserine kinase; NR, nitrate reductase; GS, glutamate synthase; GDH, glutamate dehydrogenase; HDH, histidinol dehydrogenase; P5CR, pyrroline-5-carboxylate reductase; ASS, argininosuccinate synthase; ASL, argininosuccinate lyase; GAD, glutamate decarboxylase; GHQD, 3-dehydroquinate dehydratase.

colorimetric analysis at wavelength of 620 nm, the solution contained 5 mL of anthrone and 0.5 mL of the supernatant was heated at 30 °C in a water bath for 10 min.

Soluble protein content was determined by the Coomassie Brilliant Blue G-250 method. The soluble protein content was measured by a spectrophotometer at 595 nm.

2.7. Enzyme activities of nutrition conversion

About 5 g of frozen nut tissue was ground to powder. The power was then extracted with 25 mL of phosphate-buffered saline (PBS) (pH 7.4). Then, the extract was centrifuged to take supernatant for enzyme activities determinations at 2500×g for 20 min. The enzyme activities of plant amylase, pyruvate kinase, diacylglycerol acyltransferase, acetyl CoA carboxylase, phosphofructokinase, pyruvate dehydrogenase, glyceraldehyde-3-phosphate dehydrogenase, fatty acid synthase and hexokinase were measured by using a transaminase enzyme-linked immunosorbent assay (MEIMIAN) kit (Jiangsu Meimian Co., Ltd, Jiangsu, China) and detected by microplate spectrophotometer. Enzyme activities were calculated in units according to the standard curve of the MEIMIAN kit. One unit of activity means the enzymic capacity to utilize 1 μmol of coenzyme per min at 25 °C.

2.8. Statistical and sequence analyses

Pearson's correlation coefficients (r) were calculated using SPSS (version 16.0). Amino acid sequence alignment was conducted by DNAMAN software (version 9.0). Significant differences were determined using Duncan's new multiple range test at $p < 0.05$.

3. Results

3.1. Transcriptome sequencing, assembly, and annotation

In our previous study, we found that the content of starch decreased while the content of soluble protein, soluble sugar and oil increased during post-ripening process. In addition, the effects of different temperature and humidity on the content of these substances are different (Zhang et al., 2020). In order to investigate key genes that regulate the nutrition conversion during post-ripening process of *T. grandis*, a RNA-Seq library was constructed from the RNA of seed kernels to obtain the reference transcriptome. A total of 2,817,834,612 clean reads were generated with an average Q20 of 97.01% (Supplementary Table S2). After *de novo* assembled, a total of 380,234 transcripts were generated with a mean size of 1056 bp and an average GC content of 38.23% (Supplementary Table S3). The unigene sequence length was mainly distributed between 200 and 5000 nt (Supplementary Fig. S1). These results indicated that the transcriptome sequence is credible and meets the quality requirements.

Annotation results showed that 124,111 (32.64%), 44,552 (11.72%), 13,343 (3.51%), 112,810 (29.67%), and 79,378 (20.88%) unigenes were annotated by comparing with the NR, GO, KEGG, eggNOG and

Swissprot databases, respectively (Supplementary Table S4). Almost all unigenes could be matched to a homolog in all five databases by BLASTX (Fig. 1A). The results of the similarity between the gene sequences of *T. grandis* and related species showed that the best-matched species for the gene in *T. grandis* included a 19.35% match with that of *Picea sitchensis*, 6.69% with *Amborella trichopoda*, 4.44% with *Vitis vinifera*, and 4.34% with *Picea glauca* (Fig. 1B).

In order to identify the functions of the unigenes, about 15,062 unigenes were classified into five KEGG categories, namely, molecular functions, genetic information processing, environmental information processing, cellular processes, organismal systems. Among of them, metabolism had the largest number of unigenes in which carbohydrate metabolism was the dominant group. On the other hand, environmental information processing carried the smallest unigenes which was dominated by signal transduction. (Supplementary Fig. S2A). About 18,757 unigenes were classified into GO enrichment, which included the biological process (69,658 unigenes), the molecular function (70,462 unigenes) and the cellular component (47,458 unigenes) (Supplementary Fig. S2B).

3.2. KEGG pathway enrichment analysis of differentially expressed genes (DEGs)

In order to investigate the DEGs at different temperature and humidity on *T. grandis* during the post-harvest ripening stage, the up-regulated and down-regulated genes generated from pairwise comparison were shown in Fig. 1C. In these pairwise comparisons, we detected both unique and overlapping sets of DEGs. The DEGs were followed by KEGG pathway enrichment analysis. The top 20 KEGG pathways with the highest number of DEGs are shown in Fig. 1D–G. Phenylpropanoid biosynthesis, linoleic acid metabolism, cysteine and methionine metabolism, amino sugar and nucleotide sugar metabolism, alanine, aspartate and glutamate metabolism, fructose and mannose metabolism pathways were significantly enriched in CK vs HH DEGs, which indicated that these pathways play vital roles in nutrition transformation during after-ripening under high humidity.

3.3. Identification of genes involved in nutrition conversion during post-ripening of *T. grandis*

Although most of the genes that are likely to be involved in nutrition conversion have been identified, most of those genes in *T. grandis* are still unclear. The nutrition conversion pathway of *T. grandis* was proposed according to the biosynthesis pathways of nutrition conversion in other species and the transcriptome of *T. grandis*, (Fig. 2A). A total of 861 unigenes related to nutrition conversion were identified, including 235 unigenes involved in carbohydrate synthesis, 478 unigenes involved in amino acids synthesis, and 168 unigenes involved in fatty acids synthesis (Fig. 2B).

To confirm the RNA-seq data, 5 unigenes were randomly selected from the nutrition conversion pathway, and their transcriptional abundance was estimated using qRT-PCR (Fig. 3A–E). The relative

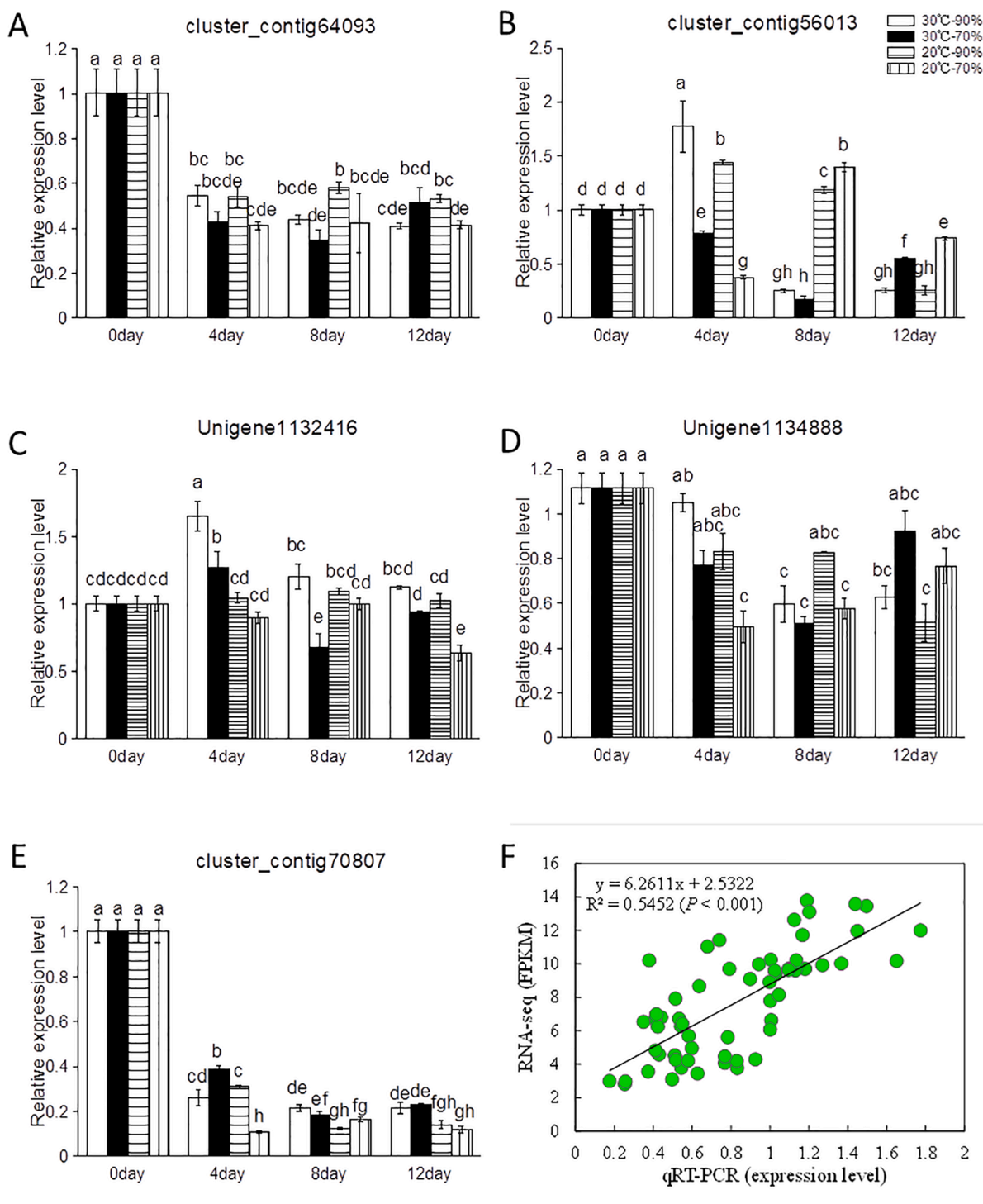


Fig. 3. The gene expression validation by qRT-PCR. (A–E) The relative transcript abundance of 5 randomly selected unigenes from the proposed nutrition conversion pathway by qRT-PCR. Different letters (a–h) indicated statistically significant difference ($P < 0.05$). (F) Correlation between qPCR and RNA sequencing for the 5 selected genes.

transcriptional abundance of these unigenes in qRT-PCR was compared with the results of RNA-seq by Pearson correlation analysis, the result showed that the qRT-PCR data was significantly correlated with the RNA-seq data with an R^2 of 0.5452 ($P < 0.001$), which indicated that the expression data from RNA-Seq was reliable (Fig. 3F).

Starch is a primary carbon and energy storage compound, and lipids are major storage products accompanied by starch degradation, which are necessary for partial lipid accumulation. As one of the famous oil plants nuts, it is the most important process to synthesis of *T. grandis* Oil.

In order to find the important unigenes encoding the enzymes involved in nutrition conversion biosynthesis pathway, we performed the correlation analysis between the content of the soluble sugar, the soluble protein, starch, oil and FPKM of all candidate genes involved in nutrition conversion biosynthesis during the post-ripening of *T. grandis*, respectively (Fig. 4A–D). We selected the unigenes with $-\log_{10}(P) \geq 2$ for further analysis. The results showed that there are 16, 26, 21 and 21 enzymes significantly correlated with starch, soluble sugar, soluble protein and total oil, respectively (Fig. 4E–H). Of these enzymes, we

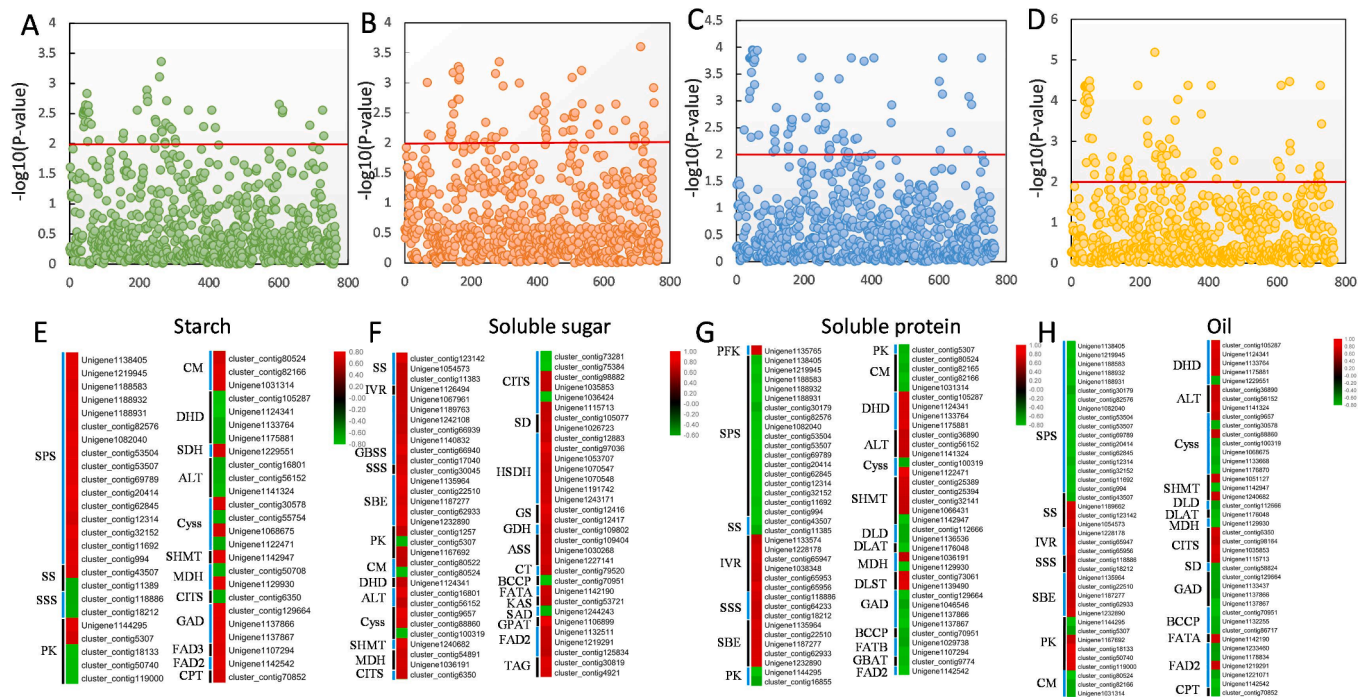


Fig. 4. The Pearson correlation analysis between the FPKM of all candidate genes involved in nutrition conversion biosynthesis and the content of the starch (A and E), soluble sugar (B and F), the soluble protein (C and G) and oil (D and H). The horizontal lines represent $-\log_{10}(p\text{-value}) = 2$. Heat map showed the correlation coefficient between the expression of unigenes and the content of nutrients at the level of $-\log_{10}(p\text{-value}) > 2$.

found that all of SS, PK, chorismate mutase (CM), 3-dehydroquinate dehydratase (DHD), alanine transaminase (ALT), cysteine synthase (Cyss), serine hydroxymethyltransferase (SHMT), malate dehydrogenase (MDH) and v-6 desaturase (FAD2) were highly and significantly correlated with the four nutrition contents. Besides, homoserine dehydrogenase (HSDH), GS, glutamate dehydrogenase (GDH), argininosuccinate synthase (ASS), ACC and ketoacyl-ACP synthase (KAS) were an extremely significant correlation with the soluble sugar, while these six enzymes have no significant correlation with other nutrition contents. Dihydrodipolyllysine-residue acetyltransferase (DLAT), DLST and FATB had significant correlation only with the soluble protein. These results implied that several main enzymes play key roles in nutrition conversion. Unigene1139490, cluster_contig119000, cluster_contig20414 and Unigene1106899 (here named as *TgGPAT1*, *TgSPS1*, *TgDLST1* and *TgPK1*, respectively) were selected for further functional analysis due to they have the highest correlation coefficients with the starch, soluble sugar, soluble protein and total oil, respectively. However, we only cloned the full CDS of *TgGPAT1*, *TgDLST1* and *TgPK1*.

3.4. Characterization and functional identification of candidate genes involved in nutrition conversion

The amino acid sequence alignment was conducted between *TgGPAT1*, *TgDLST1* and *TgPK1* and their homologs from other plants, respectively. The results indicated that *TgGPAT1* contains SCOP and PlsC domains, and these domains were highly homologous to the domains of GPATs in other plants (Fig. 5A). *TgDLST1* possesses the conserved PDB domain 3DVA (Fig. 5B). *TgPK1* was highly homologous to amyloid proteins of other plants, with a conserved SCOP domain (Fig. 5C).

To further verify the function of candidate genes, *TgDLST1*, *TgGPAT1* and *TgPK1* were transient over-expressed in tobacco leaves. Seven days after over-expression, the amounts of starch, soluble sugar, soluble protein and oil were detected in injected leaves. Over-expressed *TgPK1*, *TgDLST1* and *TgGPAT1* showed significant decreased starch content and significant increased soluble sugar and soluble protein contents

compared to wild tobacco leaves (Fig. 5D-F). However, only oil content was significantly increased in *TgDLST1* over-expressed tobacco leaves (Fig. 5G). These results suggested that *TgDLST1*, *TgGPAT1* and *TgPK1* are key enzymes contributing to nutrition conversion pathway.

3.5. Response of activities of nutrition conversion pathway enzymes to different post-ripening treatments

To further investigate the effect of protein level on the nutrition conversion of *T. grandis*, the enzyme activity was measured. The α -amylase activity under the LH treatment was significantly higher than that under the HH treatment (Fig. 6A). The nuts under the HH treatment showed a significantly higher β -amylase activity compared with the samples under the LH treatments during post-ripening (Fig. 6B). The SS enzyme activity of the T30-LH treatment was obviously higher than that of the other treatment on 4 d of post-ripening time (Fig. 6C). The nuts under the LH treatment showed a significantly higher SPS compared with the samples under the HH treatment from 4 to 12 d of post-ripening time (Fig. 6D). Except for T20-HH treatment, the IVR and GPAT activity showed an upward trend from 4 to 12 d of after-ripening time (Fig. 6E and F). The PK activity under the T30 treatment was significantly higher than that under the T20 treatment from 4 to 8 d of post-ripening time (Fig. 6G). The PDH activity under the T30-LH treatment significantly increased from 4 to 12 d of ripening time, whereas it significantly decreased under the T30-HH treatment (Fig. 6H). The DGAT activity under the T30-HH and T20-HH showed increasing trend from 4 to 12 d of after-ripening time, whereas it exhibited a significant differences between T30-HH and T20-HH from 8 to 12 d (Fig. 6I). The nuts under the T20-HH treatment showed a significantly higher HK activity compared with the samples under the T30-HH treatment on 4 d of post-ripening time (Fig. 6J). The PFK activity was significantly higher under the T30 treatment than the T20 treatment during the ripening process (Fig. 6K). The nuts under the T30-LH treatment showed a significantly higher ACC activity compared with the samples under the other treatment on 12 d of post-ripening time (Fig. 6L). FAS and transaminase activities were significantly higher under the T20 treatment than the

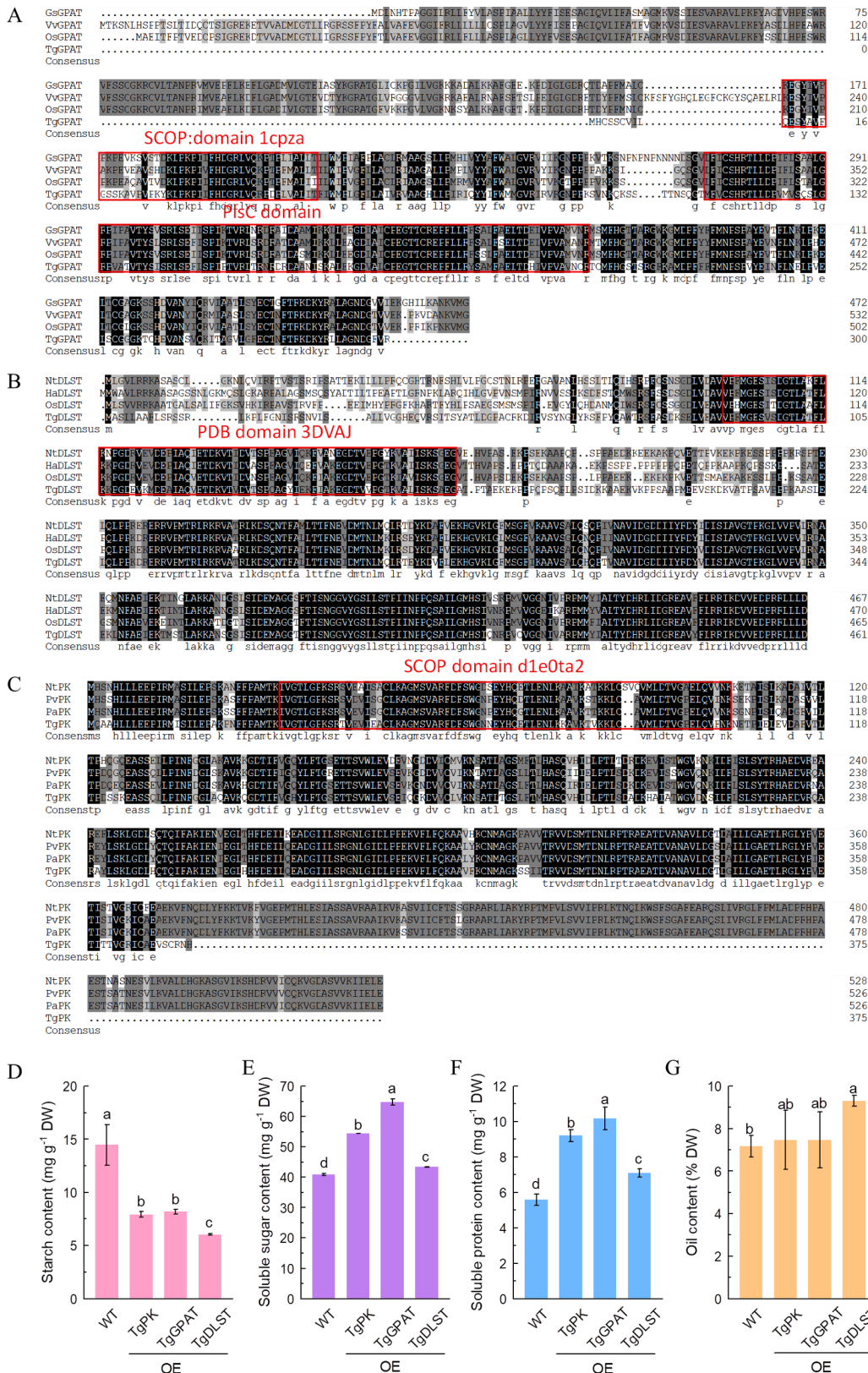


Fig. 5. Characterization and functional identification of candidate genes involved in nutrition conversion. (A-C) Amino acid sequence alignment of nutrition conversion related candidate proteins from *T. grandis* and their homologues from other plants. The following accession numbers were used: KHN05359.1: (Glycine soja); RVW46459.1: (*Vitis vinifera*); XP_022881819.1: (*Olea europaea* var. *Sylvestris*); XP_016501489.1: (*Nicotiana tabacum*); XP_022017978.1: (*Helianthus annuus*); XP_022857515.1: (*Olea europaea* var. *Sylvestris*); XP_016503432.1: (*Nicotiana tabacum*); XP_031252274.1: (*Pistacia vera*); XP_034913671.1: (*Populus alba*); (D-G) Contents of starch (D), soluble sugar (E), soluble protein (F), and oil (G) in WT and candidate genes transient over expressed tobacco leaves. WT means wild type tobacco, OE means over expression. The data indicate the mean \pm SD (n = 3). Different lowercase letters indicated statistically significant differences. ($P < 0.05$).

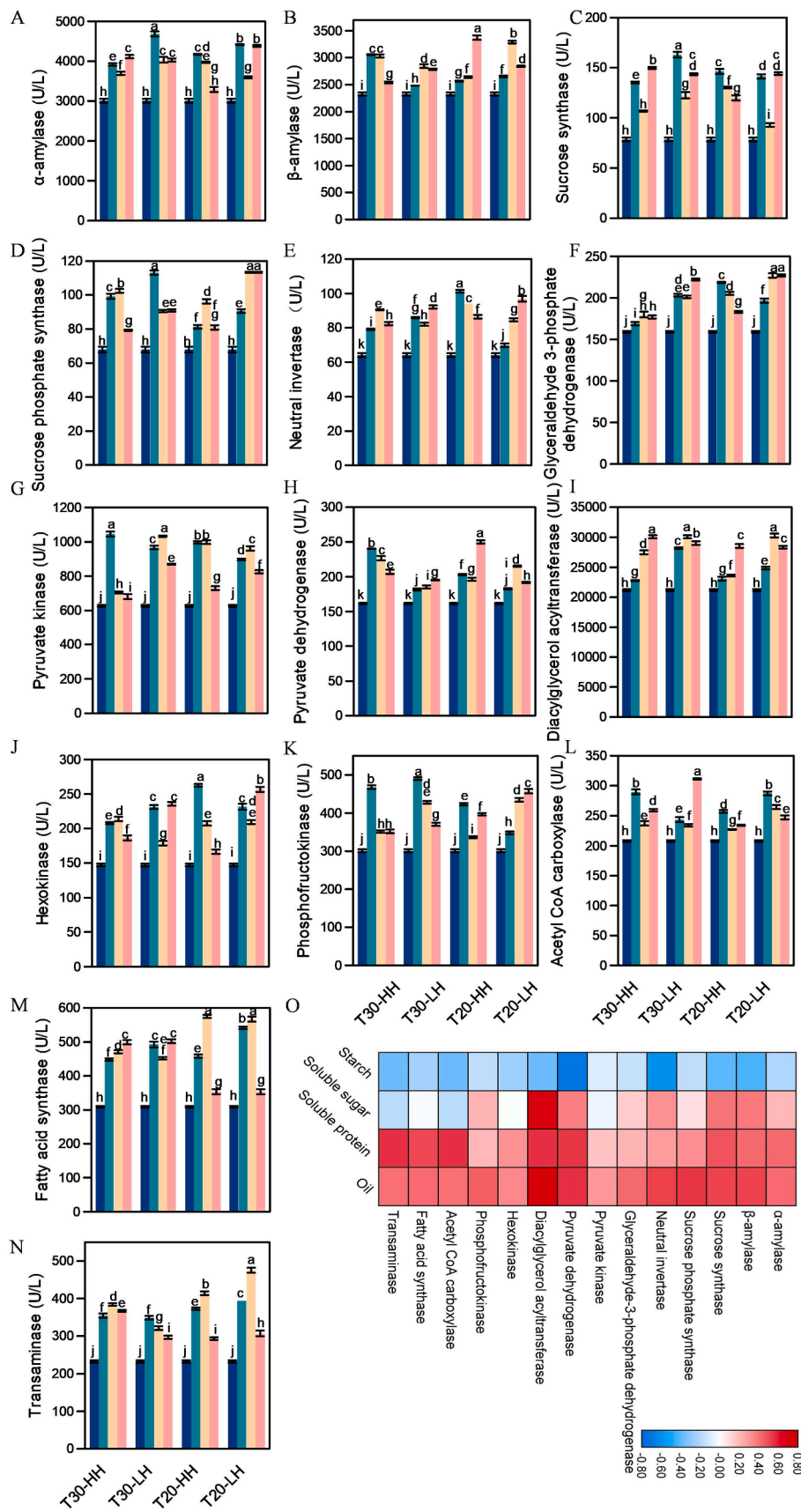


Fig. 6. Response of activities of nutrition conversion pathway enzymes to different post-ripening treatments and their correlation with Nutrient content. (A) α -amylase (B) β -amylase, (C) Sucrose synthase, (D) Sucrose phosphate synthase, (E) Neutral invertase, (F) Glyceraldehyde 3-phosphate dehydrogenase, (G) Pyruvate kinase, (H) Pyruvate dehydrogenase, (I) Diacylglycerol acyltransferase, (J) Hexokinase, (K) Phosphofruktokinase, (L) Acetyl CoA carboxylase, (M) Fatty acid synthase, (N) Transaminase, (O) Correlation analysis between enzyme activities and the content of starch, soluble sugar, soluble protein and oil. Different lower-case letters indicated statistically significant differences ($P < 0.05$).

T30 treatment on 8 d during the ripening process (Fig. 6M and N). We further made a correlation analysis between the content of starch, soluble sugar, soluble protein and oil and each enzyme activity in the nutrition conversion process. The results showed that both PDH and DGAT were significantly and positively correlated with contents of soluble protein, soluble sugar and oil, while significantly and negatively correlated with starch content, indicating that PDH and DGAT played an important role in the nutrition conversion (Fig. 6O).

4. Discussion

During the post-ripening, a coordinated and complex biochemical process continues in *T. grandis*. Several critical seed traits, such as color, texture, flavor, and aroma components could be influenced (Ye et al., 2017). Numerous factors could affect seeds quality during post-ripening and storage. Moisture content and temperature are the main factors affect seeds, resulting in changing content of starch, protein and oil (Zhou et al., 2002). During the post-ripening period, the seeds will undergo a set of progress such as embryo growth, gas exchange, changes in storage substances and enzyme activities and so on. With the elongation of the seed embryo during post-ripening, nutrition conversion was changed (Cao, 2006). The metabolism and synthesis of carbohydrates plays a vital role in nutrient conversion and energy transformation during the post-ripening. It was a very complex metabolic process, which affected the content of sugar and starch through biosynthesis, transportation, metabolism and accumulation (Dai et al., 2011). The starch was hydrolyzed into small molecules which as substrates for sugar, cellulose and protein synthesis (Ruan, 2014). Our previous study showed that starch content decreased continually in the nut during post-ripening suggesting that starch was the substrate for sugar synthesis during the post-ripening process. Similar results were reported by Silva et al. (2008), who found that starch content decreased in mango during the ripening. We also found that oil and soluble protein content increased and starch content decreased during the post-ripening process (Zhang et al., 2020). However, the molecular mechanism underlying nutrition conversion in *T. grandis* seeds during post-ripening process is still unknown. In this study, we performed transcriptome sequencing on the *T. grandis* seeds during post-ripening process to uncover the molecular basis of nutrition conversion.

Based on the transcriptome data, the metabolic pathways of nutritional transformation were further put forward. The correlation analysis between the content of the starch, soluble, protein and oil and the expression levels of unigenes indicated that SPS, GPAT, DLST and PK play important roles in the nutrition conversion. In our previous study, we found that the expression of the genes for PDAT was significantly and positively correlated with oil content in the developing seeds of different *T. grandis* landraces (Ding et al., 2020). This difference indicates that the regulatory mechanism of oil accumulation during post-ripening and development of seeds may be different in *T. grandis*. Furthermore, transient over expression of three candidate genes *TgDLST1*, *TgGPAT1* and *TgPK1* in tobacco leaves resulted in an increase in oil, soluble sugar and soluble protein contents and decreased contents of starch content. Moreover, enzyme activity analysis indicated that DGAT and PDH activity contributed to their high contents of soluble sugar, soluble protein and oil. It has been reported that sucrose biosynthesis could be promoted by the key enzyme, SPS (Huang et al., 2020). In this study, we found that the expression of some SPS unigenes was positively correlated with soluble sugar content. Furthermore, the SPS unigenes were strongly and significantly correlated with oil and soluble protein, respectively, suggesting that SPS may indirectly regulate oil and protein metabolism in *T. grandis*. It was worth noting that glycolysis is a universal pathway, which is essential for the production of oil seeds of *Arabidopsis thaliana* and oil crops (Andre et al., 2007). PK was fundamental for sustained fatty acid production in the plastids of maturing *Arabidopsis* embryos, which leads to the depletion of oil of mutant seeds, their fatty acid content was changes sharply, embryo elongation was delayed, and

ultimately, seed germination was also influenced (Sébastien et al., 2010). The high correlation between the level of transcription of PK and the content of oil suggested that PK was the key enzyme contributing to lipid biosynthesis in *T. grandis*. It has been shown that GPAT is the ER-localized enzyme responsible for plant membrane lipid and oil biosynthesis (Shockey et al., 2016). However, GPAT showed a closer connection with the content of soluble sugar in *T. grandis* than content of oil, implying GPAT may contribute more in sugar than in oil accumulation. Besides laying the foundation for a better understanding in plant nutrition conversion, the adoption of genetic engineering in exploring the potential value of the keys genes is also meaningful in providing a better strategy in regulating oil synthesis in *T. grandis*.

Up to now, little is known regarding the regulatory enzymes controlling nutrition conversion. Although previous studies have elucidated some regulatory enzymes controlling sugar, amino acids and oil biosynthesis in plants, little has been known about which enzymes could control nutrition conversion. Recently, two regulatory enzymes, PDH and DGAT, which regulate the synthesis of oil, were identified in *Arabidopsis thaliana* (Maria et al., 2012; Tovar-Mendez et al., 2002). DGAT not only catalyzed the final step of triacylglycerol but also limited to triacylglycerol accumulation in mammals, plants and microbes (Laure et al., 2014). PDH controlled the entry of carbon into the mitochondrial tricarboxylic acid (TCA) cycle to achieve cellular energy production (Ohbayashi et al., 2019). We made a correlation analysis between the content of starch, soluble sugar, soluble protein and oil and each enzyme activity in *T. grandis*, the result showed that both PDH and DGAT significantly and positively correlated with contents of soluble protein, soluble sugar and oil, while significantly and negatively correlated with starch. The high correlation suggested that PDH and DGAT were key enzymes contributing to lipid biosynthesis in *T. grandis*.

5. Conclusions

In the present study, comparative transcriptome analysis was carried out in four treatment conditions of *T. grandis*. We first proposed the nutrition conversion pathway in *T. grandis* based on transcriptome data. The potential key genes for nutrition conversion were identified by Pearson correlation analysis between the transcript abundance of pathway genes and the content of starch, soluble sugars, soluble protein and oil. Moreover, the function of candidate genes in nutrition conversion were verified through transient over-expression analysis in tobacco leaves. Results indicated that *TgGPAT*, *TgDLST* and *TgPK* play important roles in nutrition conversion. Furthermore, enzyme activity analysis indicated that DGAT and PDH activity contributed to their high contents of soluble sugar, soluble protein and oil. To sum up, this study provided the molecular basis of nutrition conversion in *T. grandis* seeds during the post-ripening stage, which will be critical for improving the quality of *T. grandis* nuts.

Declaration of Competing Interest

The authors declare that they have no known competing financial interests or personal relationships that could have appeared to influence the work reported in this paper.

Acknowledgments

This work was supported by the Key Research and Development Program of Zhejiang Province (2020C02019), the National Natural Science Foundation of China (No. 31971699), the Fundamental Research Funds for the Provincial Universities of Zhejiang (2020YQ003), the Zhejiang Provincial Academy Cooperative Forestry Science and Technology Project (2019SY07), the Scientific Research Startup Fund Project of Zhejiang A&F University (2018FR028), the Zhejiang Provincial Science and Technology Innovation Activity for College Students (2020R412049), the State Key Laboratory of

Subtropical Silviculture (ZY20180312 and ZY20180209), and the Young Elite Scientists Sponsorship Program by China Academy of Space Technology (CAST) (2018QNRC001).

Appendix A. Supplementary data

Supplementary data to this article can be found online at <https://doi.org/10.1016/j.foodchem.2022.132454>.

References

- Andre, C., Froehlich, J. E., Moll, M. R., & Benning, C. (2007). A heteromeric plastidic pyruvate kinase complex involved in seed oil biosynthesis in *Arabidopsis*. *Plant Cell*, 19, 2006–2022. <https://doi.org/10.1105/tpc.106.048629>
- Bazin, J., Langlade, N., Vincourt, P., Arribat, S., Balzergue, S., El-Maarouf-Bouteau, H., & Bailly, C. (2011). Targeted mRNA oxidation regulates sunflower seed dormancy alleviation during dry after-ripening. *Plant Cell*, 23(6), 2196–2208. <https://doi.org/10.1105/tpc.111.086694>
- Cao, B. H. (2006). Study on the after-ripening physiology and endogenous hormones of *Ginkgo biloba* seeds. *Scientia Silvae Sinicae*, 2006(02), 32–37. <https://doi.org/10.11707/j.1001-7488.20060206>
- Chapman, K. D., & Onirogge, J. B. (2012). Compartmentation of triacylglycerol accumulation in plants. *Journal of Biological Chemistry*, 287(4), 2288–2294. <https://doi.org/10.1074/jbc.R111.290072>
- Dai, N., Cohen, S., Portnoy, V., Tzuri, G., Harel-Beja, R., Pompan-Lotan, M., ... Pollock, S. (2011). Metabolism of soluble sugars in developing melon fruit: A global transcriptional view of the metabolic transition to sucrose accumulation. *Plant Molecular Biology*, 76, 1–18. <https://doi.org/10.1007/s11103-011-9757-1>
- Ding, M., Lou, H., Chen, W., Zhou, Y., Zhang, Z., Xiao, M., ... Song, L. (2020). Comparative transcriptome analysis of the genes involved in lipid biosynthesis pathway and regulation of oil body formation in *Torreya grandis* kernels. *Industrial Crops and Products*, 145, Article 112051. <https://doi.org/10.1016/j.indcrop.2019.112051>
- Giovannoni, J. (2001). Molecular biology of fruit maturation and ripening. *Annual Review of Plant Biology*, 52, 725–749. <https://doi.org/10.1146/annurev.arplant.52.1.725>
- Guilhéneuf, F., Leu, S., Zarka, A., Khozin-Goldberg, I., Khalilov, I., & Boussiba, S. (2011). Cloning and molecular characterization of a novel acyl-CoA:Diacylglycerol acyltransferase 1-like gene (*PtDGAT1*) from the diatom *Phaeodactylum tricornutum*. *FEBS Journal*, 278(19), 3651–3666. <https://doi.org/10.1111/j.1742-4658.2011.08284.x>
- Huang, T., Luo, X., Wei, M., Shan, Z., Zhu, Y., Yang, Y., & Fan, Z. (2020). Molecular cloning and expression analysis of sucrose phosphate synthase genes in cassava (*Manihot esculenta* Crantz). *Scientific Reports*, 10, 1–12. <https://doi.org/10.1038/s41598-020-77669-9>
- Laure, A., Sébastien, B., Dubreucq, B., Florent, J., & Thierry, C. (2014). Function and localization of the *Arabidopsis thaliana* diacylglycerol acyltransferase DGAT2 expressed in yeast. *Plos One*, 9(3), 192–237. <https://doi.org/10.1371/journal.pone.0092237>
- Lombardo, V. A., Osorio, S., & Borsani, J. (2011). Metabolic profiling during peach fruit development and ripening reveals the metabolic networks that underpin each developmental stage. *Plant Physiology*, 157(4), 1696–1710. <https://doi.org/10.1104/pp.111.186064>
- Lou, H., Ding, M., Wu, J., Zhang, F., Chen, W., Yang, Y., ... Song, L. (2019). Full-length transcriptome analysis of the genes involved in tocopherol biosynthesis in *Torreya grandis*. *Journal of Agricultural & Food Chemistry*, 67, 1877–1888. <https://doi.org/10.1021/acs.jafc.8b06138>
- Maria, K., Dariusz, S., Katarzyna, P., Agnieszka, W., & Justyna, T. P. (2012). DGAT2 revealed by the immunogold technique in *Arabidopsis thaliana* lipid bodies associated with microtubules. *Folia Histochemica Cytobiologica*, 50(3), 427–431. <https://doi.org/10.5603/FHC.2012.0058>
- Ni, L., & Shi, W. Y. (2014). Composition and free radical scavenging activity of kernel oil from *Torreya grandis*, *Carya cathayensis* and *Myrica rubra*. *Iranian Journal of Pharmaceutical Research*, 13(1), 221–226. PMID: 24734074.
- Ohbayashi, I., Huang, S., Fukaki, H., Song, X., Sun, S., Morita, M. T., ... Furutani, M. (2019). Mitochondrial pyruvate dehydrogenase contributes to auxin-regulated organ development. *Plant Physiology*, 180(2), 896–909. <https://doi.org/10.1104/pp.18.01460>
- Onilude, A. A., Igbinolor, R. O., & Wakil, S. M. (2010). Effect of varying relative humidity on the rancidity of cashew (*Anacardium occidentale* L.) kernel oil by lipolytic organisms. *African Journal of Biotechnology*, 9(31), 4890–4896. <https://doi.org/10.1186/1471-2180-10-208>
- Pongsawatmanit, R., Temsiripong, T., Ikeda, S., & Nishinari, K. (2006). Influence of tamarind seed xyloglucan on rheological properties and thermal stability of tapioca starch. *Journal of Food Engineering*, 77(1), 41–50. <https://doi.org/10.1016/j.jfoodeng.2005.06.017>
- Rose, J. K. C., Cosgrove, D. J., Albersheim, P., Darvill, A. G., & Bennett, A. B. (2000). Detection of expansin proteins and activity during tomato fruit ontogeny. *Plant Physiology*, 123(4), 1583–1592. <https://doi.org/10.1104/pp.123.4.1583>
- Ruan, Y. L. (2014). Sucrose metabolism: Gateway to diverse carbon use and sugar signaling. *Annual Review of Plant Biology*, 65, 33–67. <https://doi.org/10.1146/annurev-arplant-050213-040251>
- Saeed, M. K., Yulin, D., Zahida, P., Rongji, D., & Yuhong, Y. (2007). Studies on the chemical constituents of *Torreya grandis* Fort. Ex Lindl. *Journal of Applied Sciences*, 7(2), 269–273. <https://doi.org/10.3923/jas.2007.269.273>
- Sébastien, B., Sylvie, W., Dubreucq, B., Aurélie, A., & Christine, R. (2010). Function of plastidial pyruvate kinases in seeds of *Arabidopsis thaliana*. *Plant Journal*, 52(3), 405–419. <https://doi.org/10.1111/j.1365-313X.2007.03232.x>
- Shockey, J., Regmi, A., Cotton, K., Adhikari, N., Browne, J., & Bates, P. D. (2016). Identification of *Arabidopsis* GPAT9 (At5g60620) as an essential gene involved in triacylglycerol biosynthesis. *Plant Physiology*, 170(1), 163–179. <https://doi.org/10.1104/pp.15.01563>
- Silva, A. P. F. B., Nascimento, J. R. O. D., Lajolo, F. M., & Cordenunsi, B. R. (2008). Starch mobilization and sucrose accumulation in the pulp of keitt mangoes during postharvest ripening. *Journal of Food Biochemistry*, 32, 384–395. <https://doi.org/10.1111/j.1745-4514.2008.00175.x>
- Stéphane, D., Chloé, G., Mariette, A., Thierry, J., Timothy, J., Tranbarger, M. P., ... Fabienne, M. (2013). Comparative transcriptome analysis of three oil palm fruit and seed tissues that differ in oil content and fatty acid composition. *Plant Physiology*, 162(3), 1337–1358. <https://doi.org/10.1104/pp.113.220525>
- Suo, J., Tong, K., Wu, J., Ding, M., Chen, W., Yang, Y., ... Song, L. (2019). Comparative transcriptome analysis reveals key genes in the regulation of squalene and β -sitosterol biosynthesis in *Torreya grandis*. *Industrial Crops and Products*, 131, 182–193. <https://doi.org/10.1016/j.indcrop.2019.01.035>
- Tovar-Mendez, A., Miernyk, J. A., & Randall, D. D. (2002). Histidine mutagenesis of *Arabidopsis thaliana* pyruvate dehydrogenase kinase. *European Journal of Biochemistry*, 269(10), 2601–2606. <https://doi.org/10.1046/j.1432-1033.2002.02933.x>
- Wang, Q., Sun, W. J., & Bao, Y. (2017). Evolutionary pattern of the GBSS gene family in plants. *Chinese Bulletin of Botany*, 52(2), 179–187. <https://doi.org/10.11983/CBB16041>
- Wu, J. N., Ma, S., & Wang, X. X. (2017). Study on changes of carbohydrates of wheat in after-ripening stage. *Cereals & Oil*, 30(08), 11–14. in chinese.
- Xu, C., & Shanklin, J. (2016). Triacylglycerol metabolism, function, and accumulation in plant vegetative tissues. *Annual Review of Plant Biology*, 67, 179–206. <https://doi.org/10.1146/annurev-arplant-043015-111641>
- Ye, S., Wang, W. Y., Zhou, M. Y., He, Y. M., Zhuang, Z. C., Yu, W. W., Wu, J. S., Song, L. L. (2017). Effects of different harvest maturity and after-ripening ways on the harvested quality of *Torreya grandis* 'Merrillii' Seeds. *Scientia Silvae Sinicae*, 53(11), 43–51. <https://doi.org/10.11707/j.1001-7488.20171105>
- Yuan, Y., Wu, F. Z., & Zhou, X. G. (2009). Interactive effects of light intensity and nitrogen supply on sugar accumulation and activities of enzymes related to sucrose metabolism in tomato fruits. *Scientia Agricultura Sinica*, 42(4), 1331–1338. <https://doi.org/10.3864/j.issn.0578-1752.2009.04.025>
- Zhang, Z., Jin, H., Suo, J., Yu, W., Zhou, M., Dai, W., ... Wu, J. (2020). Effect of temperature and humidity on oil quality of harvested *Torreya grandis* cv. Merrillii nuts during the after-ripening stage. *Frontiers in Plant Science*, 11, 1646. <https://doi.org/10.3389/fpls.2020.573681>
- Zhou, Z., Robards, K., Helliwell, S., & Blanchard, C. (2002). Ageing of stored rice: Changes in chemical and physical attributes. *Journal of Cereal Science*, 35(1), 65–78. <https://doi.org/10.1006/jcsr.2001.0418>
- Zhou, Z., Robards, K., Helliwell, S., Blanchard, C., & Baxter, G. (2003). Rice ageing. I. Effect of changes in protein on starch behaviour. *Starch - Stärke*, 55(3–4), 162–169. <https://doi.org/10.1002/star.200390030>